Production of CH(X(2)PI) from the multiphoton dissociation of CH2CO at wavelengths of 279.3 and 308 nm

J. CHEM. SOC. FARADAY TRANS., 1994, 90(4), 523–531

Production of CH(X $^2\Pi$) from the Multiphoton Dissociation of CH_2CO at Wavelengths of 279.3 and 308 nm

Stephen M. Ball, Graham Hancock* and Mathew R. Heal†
Oxford Centre for Applied Kinetics, Physical Chemistry Laboratory, Oxford University, South Parks Road, Oxford, UK OX1 3QZ

CH(X $^2\Pi$) has been observed by laser-induced fluorescence (LIF) spectroscopy as the product of the two-photon dissociation of ketene (CH_2CO) at 279.3 and 308 nm. The nascent distribution of rotational levels is Gaussian in profile, consistent with a 'rotational reflection' principle in the dissociation. Thermodynamic arguments imply a fragmentation pathway to CH + HCO following an initial one-photon absorption to the $^1A''$ excited state of ketene, a second photon absorption, and dissociation following rearrangement *via* a formylmethylene isomer. Analysis of Λ doublets in the LIF spectra shows no orbital alignment of CH produced on photolysis at 279.3 nm, but some propensity for Π (A') symmetry alignment (π orbital of CH parallel to the plane of rotation) for photolysis at 308 nm.

The photochemistry of ketene (CH_2CO) has been widely studied, but in contrast to the wealth of investigation into the single-photon dissociation in the near UV, comparatively little work has been expended on the multiphoton dissociation channels in a similar wavelength region. Initial work concentrated on the single-photon dissociation of ketene as a major source of the methylene radical, CH_2.[1–3] Subsequent investigations of photolysis in the wavelength region 260–370 nm demonstrated the production of both the ground triplet ($\tilde{X}\,^3B_1$) and first excited singlet ($\tilde{a}\,^1A_1$) electronic states of methylene[4] with the relative yield of the excited singlet product increasing with decreasing photolysis wavelength within this near-UV region.[5] The dynamics of the process have been studied by measurements of both the CH_2 ($\tilde{a}\,^1A_1$) quantum state resolved photofragment yield spectra,[6–8] and of the CO($X\,^1\Sigma^+$) product state distributions.[9,10] Deviation of the measured excited product state distributions[11] and excited-state lifetimes[12] from those predicted by conventional phase space theory[11] have been successfully modelled by means of a variational form of the RRKM theory.[13,14] Of direct interest to the present study are measurements of the excited-state lifetimes of 19 and 130 ps for photolysis at 279 and 308 nm, respectively.[12]

Examination of ketene photolysis further into the UV has been less extensive. A rotational temperature of 6700 K for the CO fragment following photolysis at 193 nm indicates that the dissociation must proceed through a non-linear pathway.[15] Vibrationally excited CO distributions from the channel yielding CH_2 and CO have been measured by Fujimoto *et al.*[16] and Unfried *et al.*[17] These latter workers have also reported the first direct evidence for the production of the ketenyl radical from photolysis of ketene at 193 nm, clearly demonstrating a branching in the photodissociation process at this wavelength. A recent resonance Raman spectroscopic investigation by Liu *et al.*[18] for excitation wavelengths between 217 and 200 nm has confirmed the *ab initio* work of Allen and Schaeffer[19,20] that the initial dynamics of the CH_2CO $^1B_1$ dissociation proceed through an out-of-plane bend of the CCO skeleton.

In contrast to the above, information on multiphoton processes is sparse.[21–25] Although CH has been widely reported as a photofragment following irradiation of ketene in the near-UV between 285–330 nm and detection by resonance-enhanced multiphoton ionization (REMPI) with the same laser radiation, the studies have been largely spectroscopic, with little information on the dissociation dynamics. Simple energetic considerations show that to produce CH from ketene at these wavelengths requires the absorption of at least two photons. Multiphoton dissociation of other polyatomics ($CHBr_3$ at 266 nm,[26] CH_2Br_2 and $CHClBr_2$ at 248 nm [27] and CH_3I at 193 nm [28]) has long been used as a source of CH and recently there has been an attempt to characterise the nature of the multiphoton fragmentation pathway to CH from $CHBr_3$.[29] In some similar dissociations the fluorescence emission from electronically excited states of CH, when dispersed, has shown a propensity for the Π (A') Λ-doublet and further unusual rotational state dependent behaviour.[30,31] The equivalent fluorescence has recently been characterised for CH produced from multiphoton dissociation at 193 nm of ketene itself[32] and shows similar results. Rotational levels with N' from 14 to 19 in the CH ($A\,^2\Delta$) state showed higher intensity emission in the symmetric Π (A') Λ component than the antisymmetric, while the opposite was observed for levels with N' between 20 and 23.

Following a preliminary report on the kinetic measurement of the removal rate constant for CH by CH_2CO,[33] the present work details an investigation into the pathways of ground state CH(X $^2\Pi$) production from the multiphoton dissociation of ketene at wavelengths of 279.3 and 308 nm, the radical being detected by LIF spectroscopy of the $A\,^2\Delta \leftarrow X\,^2\Pi$ transition near 430 nm. From observations of the population distribution into particular CH rotational levels and the appearance of the associated Λ doubling components, the possible pathways of photolysis and of alignment in the dissociation process are discussed.

Experimental

A standard LIF detection apparatus was used for most of the work described in this paper. The CH radical was detected by on-resonance fluorescence following one-photon excitation within the Q and R branches of the CH $A\,^2\Delta \leftarrow X\,^2\Pi$ system with band origin at *ca.* 431 nm. [34] Photolysis was carried out on a static gas sample contained within an all-stainless-steel cubic reaction cell. The photolysis and probe laser beams intersected orthogonally at the centre of the cell and fluorescence was observed with an EMI 9813QKB photomultiplier tube (PMT) positioned mutually perpendicular above the intersection region. Pressures within the cell were measured using a Datametrics 0–10 Torr capacitance manometer. Photolysis radiation was obtained either from the 308 nm unpolarised output of a Questek 2240 excimer laser operating with

† Present address: School of Chemistry, University of Leeds, Leeds, UK LS2 9JT.

XeCl or, for plane polarised light at 279.3 nm, the frequency-doubled output of a QuantaRay 5200 series dye laser pumped by the Questek excimer laser. The probe laser beam was obtained variously from a Molectron Corp. UV 24 nitrogen laser pumped Molectron DL 200 series dye laser (energies up to *ca.* 50 μJ pulse^{-1}) or a Lambda Physik excimer laser–pumped dye laser combination, EMG101/FL2002, with a higher output energy. The bandwidths of these two systems were *ca.* 1.0 cm^{-1} or *ca.* 0.4 cm^{-1}, respectively, and both beams were vertically plane polarised with respect to the laboratory frame. The laser linewidths were sufficient to separate the Λ doublet transitions within a spectral scan but insufficient in general to resolve fully the spin–orbit components. Typical laser pulse rate was 10 Hz.

The probe laser beam was passed through long side arms which contained a series of baffle rings and Brewster-angled windows in order to minimise scattered light that might otherwise be viewed by the PMT. This was of particular importance in these experiments since fluorescence was always detected on-resonance with the exciting radiation. A short focal length quartz lens ($f = 22$ cm) focussed the photolysis radiation into the centre of the cell. In the case of the 279.3 nm radiation, for which the photolysis beam was also polarised, two distinct relative polarisation geometries of photolysis–probe beam could be used; first, the electric vector of both beams parallel to each other and vertically orientated with respect to the laboratory frame and secondly, with the polarisation of the photolysis beam rotated through 90°.

Fluorescence was imaged onto the PMT with a further series of lenses and baffle rings and passed through an interference filter. The PMT signal was fed either into a 20 MHz Thurlby DSA524 digital storage adaptor and thence to a PC, or was gated and integrated using a Brookdeal 9415 linear gate and 9425 scan delay generator combination. The output was taken to a chart recorder. Triggering of all electronic equipment and both lasers was effected by a home-built pulse-delay generator capable of delivering a sequence of four variable delay pulses. Experiments were performed at a ketene pressure of ⩽30 mTorr with a delay between dissociation and probe lasers of ⩽0.3 μs. The measurement of fluorescence lifetimes utilised the 50 Ω input of a 20 MHz digitising board of the PC (Markenrich Corp. WAAG card) capable of averaging over several thousand laser shots.

The ketene precursor (CH_2CO) used in all experiments was prepared by the pyrolysis of acetone vapour passing over an electrically heated nichrome element at *ca.* 650 °C in a stream of inert He carrier gas.[35] The ketene was purified by distillation at 195 K (trichloroethylene–dry ice slush bath), trap-to-

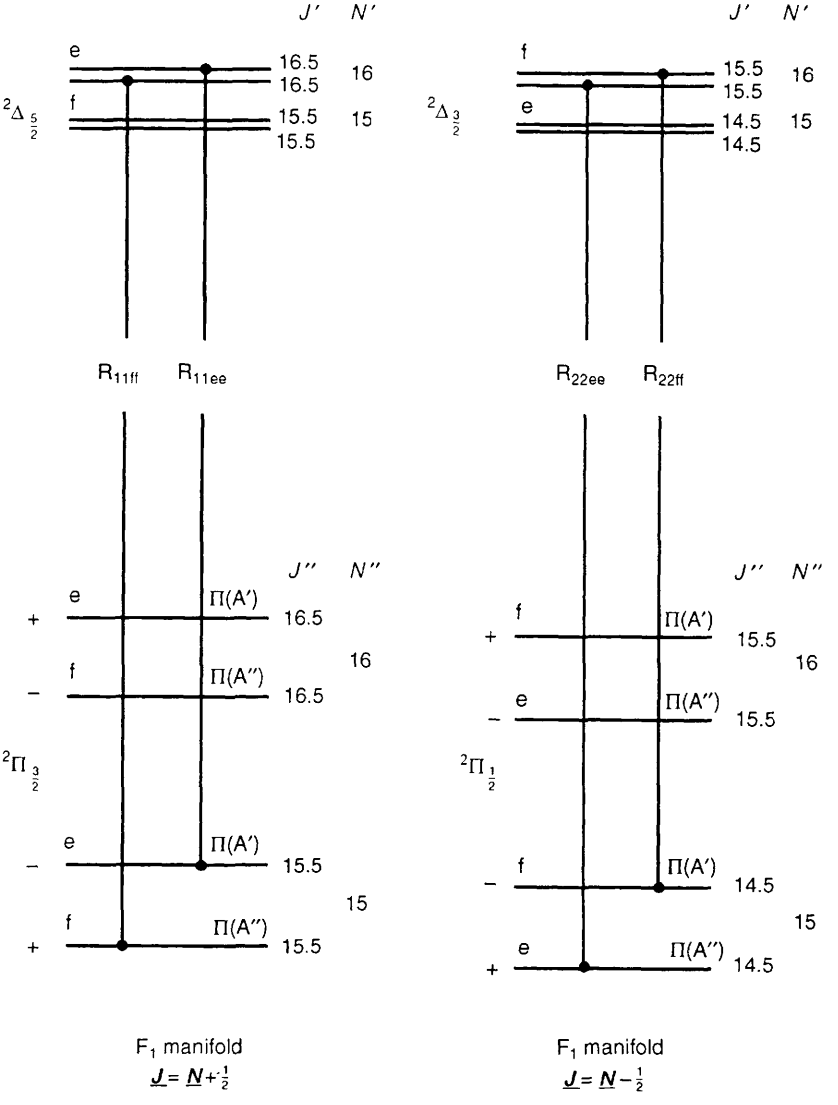

Fig. 1 Rotational energy level diagram for CH illustrating the nomenclature of the energy levels and an example of the four allowed R-branch transitions for a given value of N'' within the $A\,^2\Delta$–$X\,^2\Pi$ band

trap distillations at 77 K and continuous pumping on the product at 113 K using an isopentane–liquid-nitrogen slush bath. Sample purity was confirmed on each occasion by mass spectrometric analysis and UV absorption between 200 and 400 nm with cross-section at a maximum of 2.0×10^{-20} cm^2.[36] During experiments the ketene was stored at pressures less than 20 Torr in a darkened bulb to prevent polymerisation.

CH Spectroscopy

The ground state of CH($X\,^2\Pi$) is subject to both Λ doubling and spin–orbit splitting. The spin–orbit parameter is sufficiently small compared with the rotational constant ($A = 28.14$ cm^{-1},[34] $B_e = 14.46$ cm^{-1} [37]) to ensure that it approaches Hund's case (b) at relatively low values of the total angular momentum quantum number J''. Fig. 1 illustrates the energy levels involved. Spin–orbit splitting creates two manifolds of levels designated F_1 ($J'' = N'' + \frac{1}{2}$) and F_2 ($J'' = N'' - \frac{1}{2}$), where N'' is the total angular momentum excluding spin. Λ doubling produces splittings in each of these J'' levels, to give states of + and − symmetry and the labelling of these levels with respect to inversion of all coordinates follows the convention of Brown *et al.*[38] For a Hund's case (b) molecule such as CH($X\,^2\Pi$) all lower levels of each Λ doublet pair in the F_1 spin–orbit manifold are designated by the notation f, whereas in the F_2 manifold the lower components all constitute a series of e levels. The levels can be additionally classified according to the behaviour of the electronic wavefunction on reflection in the plane of rotation in the limit of high J. As the case (b) limit is approached the F_{1e} and F_{2f} wavefunctions of a $^2\Pi$ state acquire symmetric character with respect to the reflection while the F_{1f} and F_{2e} wavefunctions acquire antisymmetric character. Current notation[39] describes these levels as being of Π (A′) or Π (A″) symmetry, respectively, for all values of J. Observation of preferential population in one of the Λ doublets can yield important information on the dynamics of a dissociative or reactive process, provided there is complete alignment of the pπ electron lobe parallel or perpendicular to the total angular momentum vector $\boldsymbol{J}$ at a given value of quantum number J. For the case of CH($X\,^2\Pi$), this degree of electron alignment rapidly approaches its limiting value of unity at relatively low values of J ($\gtrsim 4.5$)[40] so that any propensity in Λ population can be ascribed directly to dynamical effects.

The first excited state of CH ($A\,^2\Delta$) is also subject to a Λ-type doubling, but its effect, and that of spin–orbit coupling ($A = -1.1$ cm^{-1} [34]) are both small in comparison with the ground-state behaviour. The selection rules[38] dictate that absorption transitions from the ground state to the first excited state are allowed from all four of the rotational levels taking the same lower quantum number N'' and these form a closely spaced quartet in the spectrum, although at high values of N'' the Λ splitting dominates considerably over the spin–orbit splitting which may not be fully resolved. Fig. 1 illustrates the four allowed R-type transitions for $N'' = 15$ of the A–X spectrum. It is important to note, however, that both the closely spaced transitions of spin–orbit origin within one pair of the Λ doublet (for example R_{11ee} and R_{22ff}) together probe the population of CH levels having Π (A′) symmetry, while the closely spaced transitions R_{11ff} and R_{22ee} together probe population of CH having Π (A″) symmetry. The relative populations of CH in these two symmetries are therefore determined directly from a limited LIF scan of one group of R branch (or P branch) transitions arising from a single value of N'', in contrast to similar studies for the OH ($X\,^2\Pi$) radical.[41]

Results and Discussion

The original aims of the present experiments were to try to devise a method of detection of ground-state methylene radical, $CH_2(\tilde{X}\,^3B_1)$, by two-photon excitation of the upper predissociated $^3A_2$ state followed by LIF detection of the expected CH($X\,^2\Pi$) product. Ketene was photolysed at 308 nm to produce $CH_2(\tilde{a}\,^1A_1)$, which was then quenched to the ground state by collisions with Ar. At a suitable delay the two-photon excitation radiation at either 279.3 nm or 282.9 nm was fired into the cell in an attempt to form the $^3A_2$ state, these wavelengths being those expected for excitation of the (0, 1, 0) or (0, 0, 0) levels. In the event copious CH LIF signals were observed with a single UV wavelength (308, 279.3 or 282.9 nm) directed into the cell, and no additional formation of CH($X\,^2\Pi$) from the route

$$CH_2CO \xrightarrow{308} {}^1CH_2 + CO$$

$$^1CH_2 + Ar \longrightarrow {}^3CH_2 + Ar$$

$$^3CH_2 \rightarrow \rightarrow CH_2(^3A_2) \rightarrow CH(X\,^2\Pi) + H$$

could be detected. Furthermore, strong emission from electronically excited CH was detected in the $A\,^2\Delta$–$X\,^2\Pi$ and $B\,^2\Sigma$–$X\,^2\Pi$ bands near 430 and 390 nm following ketene photolysis at all three wavelengths. As the A–X emission was at the same wavelength as the LIF used to detect ground-state CH, conditions were sought to minimise this contribution which appears as background in the LIF spectrum. Both the A state emission and the LIF signals exhibited the same quadratic dependence on photolysis laser intensity, and thus this parameter was ineffective in maximising the signal to background ratio: this point will be further considered when the mechanism for formation of the excited state of CH is discussed. However, the photolysis wavelength dependence of the signals differed markedly, as illustrated in Fig. 2. At 279.3 nm it can be seen that the signal to background ratio is near its maximum value, and hence this wavelength was chosen for the majority of the studies of the dissociation dynamics where short time delays were required between dissociation and probe laser pulses. Further studies at 308 nm were facilitated by the better energy stability of the excimer laser output compared with that of the frequency doubled layer dye laser.

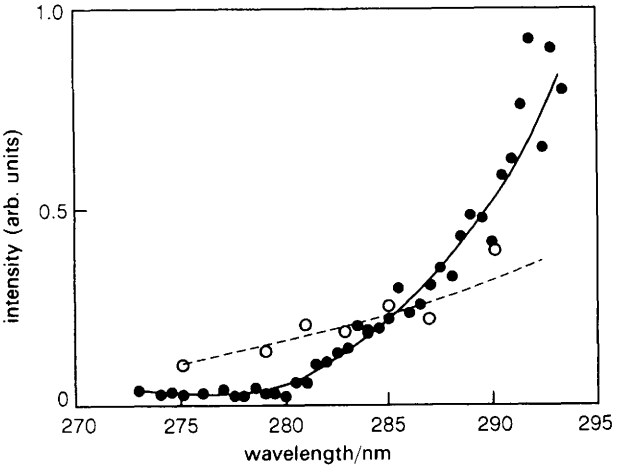

Fig. 2 The variation with photolysis wavelength of the LIF signal at the Q-branch head of the CH $A\,^2\Delta \leftarrow X\,^2\Pi$ band (○) and of the nascent CH emission recorded at the peak of the $A\,^2\Delta \rightarrow X\,^2\Pi$ band [(●) and solid line]. Both fluorescence signals have been corrected for a quadratic dependence on photolysis intensity. The single-photon absorption spectrum of ketene in the same wavelength region is shown as a dashed line for comparison.

Thermodynamics of Photodissociation

The presence of ground-state CH was unequivocally identified by assignment of the transitions within the LIF spectra with reference to the compilation of Moore and Broida[42] and Bembernek *et al.*[34] and spectra recorded for R-branch transitions following photolysis at 279.3 nm and 308 nm are shown in Fig. 3 and 4, respectively. The magnitude of the LIF signal was measured as a function of dissociation laser intensity at 279.3 nm, both at the Q branch head of the CH $A\,^2\Delta \leftarrow X\,^2\Pi$ band at 431.7 nm and at the unresolved spin–orbit shorter Λ wavelength component [probing total Π (A″) symmetry] of the $N'' = 10$ R-branch transition at 424.9 nm. In both instances a value of $n = 1.9 \pm 0.1$ for a dependence of the form I^n indicates a dissociation process to yield $CH(X\,^2\Pi)$ that requires the absorption of at least two photons at a wavelength of 279.3 nm. Thermodynamic heats of formation data[43,44] dictate that the following two fragmentations are both energetically accessible pathways for production of CH.

$$CH_2CO(X\,^1A_1) \rightarrow CH(X\,^2\Pi) + HCO(\tilde{X}\,^2A'); \quad \Delta H_0^0 = 56\,726 \pm 838\ cm^{-1} \quad (1)$$

$$CH_2CO(X\,^1A_1) \rightarrow CH(X\,^2\Pi) + H(^2S) + CO(X\,^1\Sigma^+); \quad \Delta H_0^0 = 61\,664 \pm 184\ cm^{-1} \quad (2)$$

The total energy supplied by absorption of two photons at 279.3 or 308 nm is equal to 71 608 or 64 935 cm^{-1}, respectively, which is sufficient in both cases to exceed the thermodynamic thresholds of both the above fragmentations.

It is reasonable to assume that the dissociation processes leading to formation of $CH(X\,^2\Pi)$ are the result of absorption of no more than two photons at the wavelengths used, by application of the following arguments. An observed quadratic dependence on laser intensity would necessitate that one absorption step be fully saturated for all laser fluences investigated if the photodissociation required absorption of more than two photons. Well documented work as cited in the introduction has established that absorption of one photon in the near-UV readily excites ketene to its $^1A''$ surface during dissociation to $^1CH_2$ and CO products. Under our experimental conditions, the 380 nm excimer beam of 80 mJ $pulse^{-1}$ focussed to a minimum beam diameter of 3 mm supplies a maximum photon density of $1.7 \times 10^{18}\ cm^{-2}$. An absorption cross-section of $2 \times 10^{-20}\ cm^2$ for CH_2CO at this wavelength[36] indicates that this transition is far from saturated, and this was confirmed by measurements of a linear dependence for $^1CH_2$ formation, observed by LIF of the $^1B_1$ (0, 16, 0) $\leftarrow$ $^1A_1$(0, 0, 0) transition at 537.5 nm, on 308 nm laser energy. Photon densities at 279.3 nm were also calculated to be below the ketene saturation limit.

Direct population of this real molecular eigenstate will thus be the predominant absorption process of the first photon, but for subsequent absorption, photofragmentation of the $^1A''$ state must now compete. At the photon intensities used (*ca.* 2×10^{26} photons $cm^{-2}\ s^{-1}$), the second photon absorption cross-section at 279.3 nm must be *ca.* $10^{-16}\ cm^2$ to compete with the (relatively slow) ketene dissociation rate of $5.3 \times 10^{10}\ s^{-1}$.[12] This high cross-section (considerably higher than that for absorption of the first photon) is probably not achieved for absorption from the $^1A''$ state, and implies that a second absorption process is again not saturated. At 279.3 nm, two-photon absorption to Rydberg states (which might live long enough to absorb further) is not seen in REMPI studies of ketene[25] (although a weak feature is observed near 308 nm) and thus non-saturated absorption probably leads to a dissociative level above the thermodynamic threshold to form CH. Further absorption cannot be ruled out, but must be saturated, which from a presumed completely dissociative state is an unlikely event; coherent two-photon absorption from the $^1A''$ state is ruled out because of the observed quadratic energy dependence.

As dissociation of the $^1A''$ intermediate state almost certainly predominates over further absorption, we need to consider the formation of CH from the dissociation of the $^1CH_2$ intermediate. This can only take place with the first absorp-

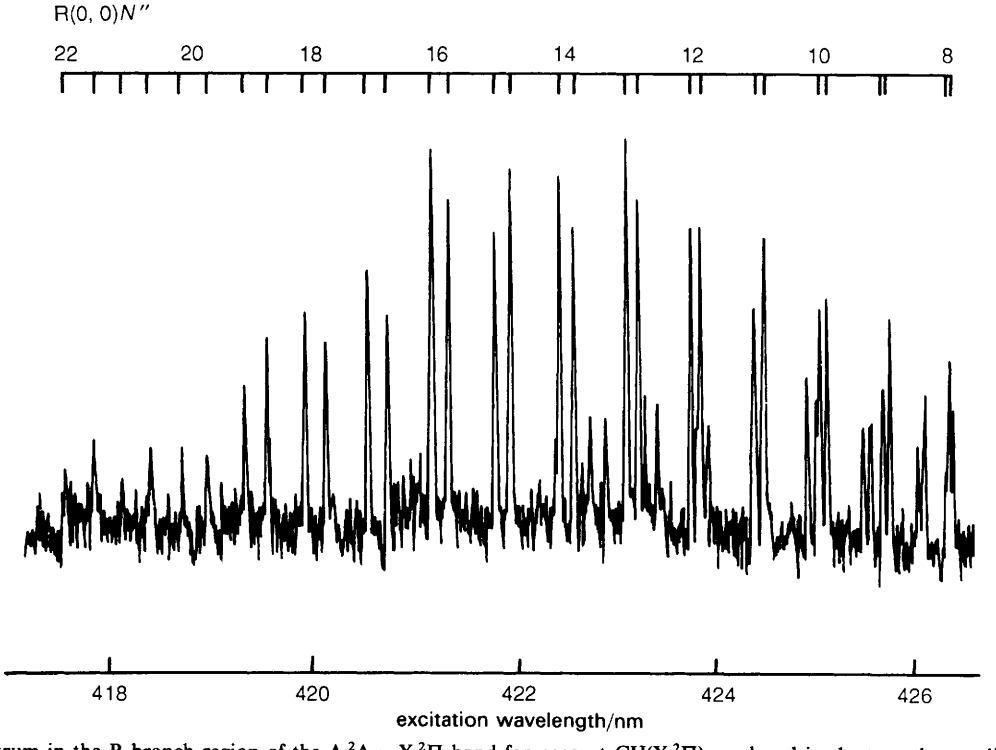

Fig. 3 LIF spectrum in the R-branch region of the $A\,^2\Delta \leftarrow X\,^2\Pi$ band for nascent $CH(X\,^2\Pi)$ produced in the two-photon dissociation of 23 mTorr ketene at 279.3 nm using the Molectron nitrogen laser pumped dye laser combination as probe at a delay of <0.3 μs. Positions of the R-branch transitions in the (0, 0) band are indicated as a function of N''.

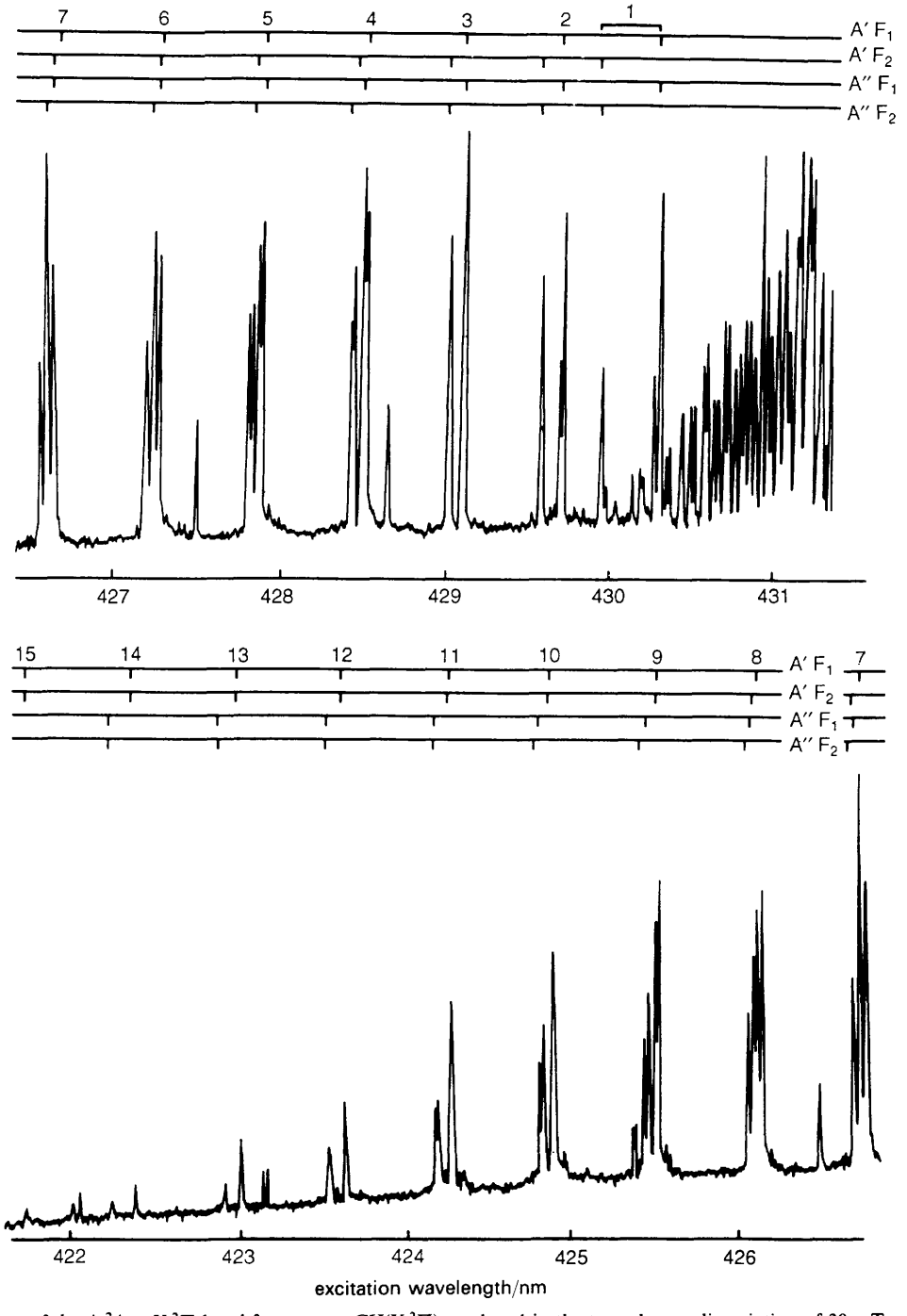

Fig. 4 LIF spectrum of the $A\,^2\Delta \leftarrow X\,^2\Pi$ band for nascent $CH(X\,^2\Pi)$ produced in the two-photon dissociation of 30 mTorr ketene at 308 nm using the narrow band Lambda excimer laser pumped dye laser combination as probe at a delay of <0.3 μs. Positions of the R-branch transitions originating from the four levels associated with each N'' value are indicated.

tion step of $^1CH_2$ being to a real eigenstate: no absorption features at these UV wavelengths have been observed in the electronic spectra of $^1CH_2$.[45] The excess energy at 308 nm above the singlet threshold for dissociation into $^1CH_2$ and CO (measured spectroscopically as 30116.2 cm^{-1} [7]) is 2351 cm^{-1}. Molecular beam studies of Hayden *et al.*[9] have demonstrated that an average fraction of 0.33 of this excess energy is channelled into product translation, $\langle E_{trans} \rangle$. When the average fractions of excess energy partitioned into CO rotation and vibration are included, 0.08 and 0.40, respectively,[10] only 19% of available energy is apportioned to internal modes of $^1CH_2$. This amounts to 632 cm^{-1} when the internal energy of ketene at room temperature (450 cm^{-1})[10] is included in the dissociation. The enthalpy of dissociation for CH_2 ($\tilde{a}\,^1A_1$) into $CH(X\,^2\Pi)$ and $H(^2S)$ is 31348 ± 36 cm^{-1} and from this is derived an excess energy of only 920 ± 36 cm^{-1} after absorption of a second photon at 308 nm, and thus a maximum of 1452 cm^{-1} for the average energy available for disposal to the CH + H fragments. The observed peak of $N'' = 6$ ($E_{rot} \approx 580$ cm^{-1})[46] for the CH nascent rotational distribution would therefore imply a minimum value of 40% for the average fraction of the excess energy in the second photolysis step that would be given to CH rotation. This value is sufficiently unrealistic for such a process to be rejected. For comparison, in the photodissociation of H_2O, a bent dihyride with a bond angle similar to $^1CH_2$, average energy fractions patitioned into OH rotation have been measured at only 2%[41,47,48] or 3%[49] for

dissociation at 157 nm or 193 nm, respectively. Similarly only 3% of the excess energy is associated with rotation of the NH fragment in the dissociation of HN_3 at 266 nm.[50]

Analogous thermodynamic arguments further demonstrate that a two-photon dissociation to CH + H + CO products directly is rather less probable than to CH + HCO products again on the basis of observed populations of CH rotational levels, quite apart from the lower probability of a three-body fragmentation. The excess energy of *ca.* 3720 cm^{-1} (including internal energy of bulk room-temperature ketene) for the former pathway at 308 nm just permits population of the $N'' = 16$ rotational levels with $E_{rot} \approx 3740$ cm^{-1} [46] to be an allowed product state. The observed LIF spectrum at 308 nm shows some evidence for population of the $N'' = 15$ doublet above the baseline noise. Although this is not inconsistent with energetics of dissociation to CH + H + CO, it would require that for some proportion of the dissociation processes virtually the entire excess energy be channelled solely into CH rotation. This is intuitively unreasonable for a process which ultimately yields three co-fragments, all three of which are expected to possess translational energy and (in the case of CH and CO) vibrational and rotational energy. Consideration must also be given to whether population of such high rotational levels of CH is consistent with an overall conservation of angular momentum, either through rotation of the CO co-fragment or through total orbital angular momentum of the products. Rotation of CO ($B_e = 1.93$ cm^{-1} [51]) with a similar number of quanta necessitates additional energy of *ca.* 460 cm^{-1} to be added to that associated with $^1CH_2$ rotation. For dissociation at 279.3 nm the highest observed level is $N'' = 22$ (Fig. 3) and in this case this corresponds to 70% of the available energy in the three-body fragmentation appearing as CH rotation, again considered to be unlikely.

We may therefore conclude that dissociation of ketene at the wavelengths investigated must occur through a sequential two-photon absorption (within the photolysis pulse width of 10 ns) where absorption of a second photon from the intermediate electronic state competes effectively with unimolecular dissociation to $^1CH_2$ + CO fragments. We note that the close similarity between the photodissociation yield spectrum of CH($X\,^2\Pi$) and the ketene one-photon absorption cross-section is probably fortuitous, as over the wavelength range 279–290 nm the $^1A''$ intermediate-state lifetime increases by a factor of 2 [12] and this would imply a larger fraction of molecules absorbing in the second step. Reduction of the second absorption cross-section by a similar factor could counter this effect.

The production of CH as a fragment invokes a rearrangement to a formylmethylene HCCHO isomer of CH_2CO, a process which must be accomplished on a timescale comparable to internal conversion. The single-photon dissociation is relatively slow with measured lifetimes of 130 and 19 ps at 308 and 279 nm, respectively,[12] consistent with a significant intramolecular energy redistribution into the reaction coordinate of the polyatomic before fragmentation.[52] Several experiments have demonstrated that ketene will undergo isomerisation reactions. Russell and Rowland[53] photolysed ketene labelled at the methylene carbon and measured significant yields of ^{14}CO, while in a separate study Montague and Rowland[54] observed carbon exchange in the reaction of labelled singlet methylene, $^{14}CH_2$ ($\tilde{a}\,^1A_1$), with CO, also to yield ^{14}CO as a product. The symmetric O-bridged oxirene has been postulated as an intermediate. More recently a thorough investigation into the kinetics of intramolecular carbon exchange in ketene by Lovejoy *et al.*[55] has concluded that the isomerisation of ketene does compete effectively with unimolecular dissociation. RRKM calculations using an oxirene transition state are in quantitative agreement with the experimental rate constants for most of the energy range studies (up to 4000 cm^{-1} above the singlet methylene dissociation threshold). In the context of the present work it is important to note that rearrangement of ketene to an oxirene species must proceed through a 1,2-hydrogen shift as a first step leading to formation of formylmethylene as an intermediate species. Carbon-atom exchange by rearrangement through an oxiranylidene intermediate is energetically unfavourable because of the extremely high barrier (489 kJ mol^{-1} above ground-state ketene) which lies along the reaction coordinate between these two isomers.[56,57] In contrast, the same *ab initio* calculations[56,57] show there to be an energy separation of only 310 kJ mol^{-1} between ketene and formylmethylene and only a very small energy barrier towards subsequent oxirene ring formation, although more recent high-level calculations by Vacek *et al.*[58] have suggested that, at yet higher levels of theory, oxirene may be reduced to a transition state only. These latter workers were also unable to locate any transition state separating oxirene and formylmethylene and concluded that formylmethylene was unstable, in agreement with Tanake and Yoshimine.[57]

Nascent CH($X\,^2\Pi$) Rotational Distributions

The data of Fig. 3 and 4 were converted into relative rotational populations as a function of N'' using the standard procedure, taking account of the laser intensities (a linear variation of LIF signal with probe laser energy was established) and detection sensitivities, but neglecting any polarisation terms arising from fragment alignment. The latter effects are expected to be small and experiments to probe this, in which relative polarisations of probe and photolysis lasers were varied, showed no observable spectral differences. Rotational line strengths were calculated from the formulae derived by Mulliken.[59] CH $^2\Delta$ radiative lifetimes have been shown to be invariant for $v' = 0$ at N' levels between 6 and 23,[60] and thus populations derived by LIF in this work were not influenced by predissociation of the upper state. An experimental check on the radiative lifetimes at the Q branch head and on all four Λ doublet and spin–orbit components of the $N' = 16$ level showed values of 550 ± 40 ns, consistent with previously reported measurements.[60–63] For excitation at 279.3 nm the resultant populations shown in Fig. 5 are averages over the two spin–orbit states for a given N'', but are clearly separated into Π (A′) and Π (A″) components for the levels measured (N'' between 8 and 22).

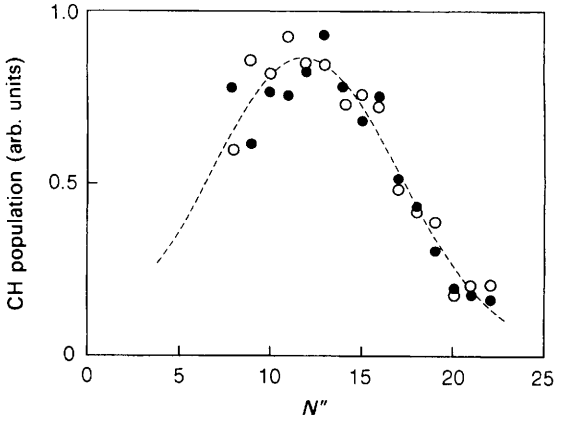

Fig. 5 Relative rotational populations as a function of N'' of the nascent CH($X\,^2\Pi$) ground-state levels corresponding to the spectrum of Fig. 3 for photolysis of 23 mTorr of ketene at 279.3 nm. (○) Levels of Π (A′) symmetry, (●) Π (A″) symmetry. The dashed line is the best-fit Gaussian to both Λ doublet components of the distribution.

The spectrum indicates that both Λ doublets show equal population for N'' levels probed, and this was checked by careful slow scans at higher resolution over the selected spectral region. For $N'' = 10$, 15 and 18 the ratio Π (A″) : Π (A′) was found to be 1.05 ± 0.12, 0.98 ± 0.10 and 1.0, with error bars here showing deviation from the mean of a number of experiments (a single run in the case of $N'' = 18$).

As can be seen in Fig. 4, the observations at lower N'' for photolysis at 308 nm (carried out with the higher-resolution excimer pumped dye laser) allowed resolution, in some cases, of all four R branch lines. Fig. 6 shows the population of the A′ F_1 levels over J'' values from 1.5 to 12.5, these representing the levels which could be resolved from their neighbours over the widest range of J''. Clearly apparent from the spectrum in Fig. 4 is that now the Λ doublets are not of the same intensity (although care must be taken in interpreting peak heights in these cases as equivalent to populations). Again scans over the areas of the relevant peaks now show values of Π (A″) : Π (A′) of 0.63 ± 0.04 for $N'' = 10$ and 0.86 ± 0.06 for $N'' = 12$.

The distributions at the two wavelengths show Gaussian forms, peaking at $N'' = 12$ and $J'' = 7.5$ for photolysis at 279.3 and 308 nm, respectively, corresponding to average fractions of 17% and 7% of total excess energy partitioned into rotation for the two-photon dissociation producing CH and HCO fragments. Further experimental results at 279.3 nm in which an excimer pumped dye laser was used (at higher resolution than the data of Fig. 3) as the LIF source, and for which different detector sensitivities applied, showed essentially the same Gaussian distribution (and confirmed the low population in low N'' levels). Fig. 3 also shows some evidence of weaker signals from $v'' = 1$ in CH (for example the doublets between those illustrated for $N'' = 8$ and 9 in the 0,0 band) but low signal to noise levels precluded full analysis. It should however be noted that these are absent in the 308 nm case. As Franck–Condon factors and detection sensitivities for the 1,1 and 0,0 bands are similar, it can be concluded that these vibrational levels are certainly not inverted, and the fraction leading to vibrational excitation in CH is low.

A Gaussian-shaped distribution amongst rotational levels is indicative of a 'rotational reflection principle'[64] where there is a strong final-state interaction in the exit channel on the excited state potential V_{ex} accessed immediately after the absorption process. According to the Franck–Condon (FC) principle, the absorption step to V_{ex} defines an initial probability $P_0(e, v, j)$ which is modified by the intermolecular forces induced by the excited state potential as the molecule dissociates. In a direct photodissociation where the final-state interaction is zero or very weak (the FC limit) the initially prepared distribution of angular momentum states j is not changed during fragmentation and the final rotational state distribution is a simple map of the initial parent wavefunction. When a strong final-state interaction exists, the initially prepared distribution is more or less completely destroyed and the final-state distribution becomes a direct map of the anisotropy of V_{ex} around the ground-state equilibrium,[65] *i.e.* the final-state distribution is roughly a reflection of the ground-state bending wavefunction of the bond being broken with probability proportional to the square of the modulus of the bending angle. (Each final rotational state is essentially determined by one initial angle.) Since the dissociation of ketene into CH *via* a two-photon absorption cannot be a direct process from a repulsive surface, the final-state distribution of CH must be predominantly determined in the exit channel and all memory of the CH_2CO initial-state distribution destroyed. This is the case for the dissociation of formaldehyde, H_2CO, into H_2 and CO in the near-UV[66] or the photolysis of H_2O_2 at 193 nm.[67] In both these examples, the energy associated with the peak centres of the Gaussian CO and OH rotational distributions corresponds to *ca.* 15–20% of the total available excess energy and these are similar fractions to those observed in our CH distributions. However, in order to model the dynamical photodissociation mapping fully in this instance it is crucial to know the exact details of the excited-state potential-energy surface (PES), V_{ex}, information which is unavailable at present for a two-photon absorption in ketene. The less clearly defined Gaussian-shaped rotational distribution following photolysis at 308 nm may be a consequence of the predicted energy dependence for these distributions in the strong coupling limit[64] owing to access of different regions of anisotropy in the excited PES. Alternatively, it is possible that in this absorption region FC mapping as well as dynamical mapping may overlap or that the two-photon ketene dissociation system may be complicated by the involvement of more than one excited state as has been inferred in the photodissociation of OCS.[68]

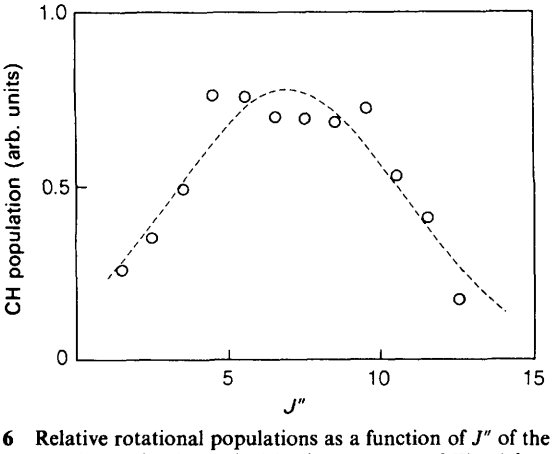

Fig. 6 Relative rotational populations as a function of J'' of the CH A′ F_1 ground-state levels marked in the spectrum of Fig. 4 for photolysis of 30 mTorr ketene at 308 nm. The dashed line is the best-fit Gaussian to the component state distribution.

Orbital Alignment of CH

The nascent CH produced in two-photon phytolysis of ketene of 279.3 nm clearly shows that for high values of N'' ($\geqslant 10$), where spin–orbit coupling is small, both symmetry components of each Λ doublet are equally populated to within a reasonable experimental error. The degree of electron alignment for the CH radical indicates that alignment of the π orbital parallel or perpendicular to $\boldsymbol{J}$ occurs at relatively low values of J. Therefore any observed propensity in Λ doublet population or change in propensity with increasing J (or N) may be ascribed to a dynamical effect in the photodissociation process. No such effect is observed. Furthermore these ratios were invariant to a 90° change in the plane of polarisation of the linearly polarised probe laser beam relative to the plane of polarisation of the photolysis laser beam in the laboratory frame. This lack of polarisation dependence does not provide any direct information on the stereochemical dynamics of the photodissociation. When the parent molecule is photoselected by the polarised laser beam, the optical transition moment $\boldsymbol{\mu}$ (linked to the molecular framework) is preferentially aligned along the $\boldsymbol{E}$ vector of the exciting radiation. This establishes a stereochemical relationship between the direction of the orbital correlating to the π orbital of the outgoing diatomic and the rotating impulsive imparted to it by the fragmentation. The photolysis of *trans*-HONO at 350 nm to produce OH with Λ doublets preferentially populated in Π(A′) symmetry (π orbital parallel to plane of rotation)[69] or the photolysis of methyl nitrite,

CH_3ONO, at 364 nm,[70] or of cold water in its first absorption band at 157 nm[41] both yielding $^2\Pi$ diatomics with preferential population in II (A″) symmetry, are all excellent examples of this stereoselectivity. However, when the fragmentation process is slower than out-of-plane molecular rotation the transfer of preferential alignment from parent to products will be lost and consequently no dependence on relative photolysis–probe polarisation geometries will be observed. In the experiments described here a bulk sample only of ketene (at $T \approx 298$ K) was probed. The rotational constants of ketene have been determined both from microwave and infrared spectroscopy[71] and *ab initio* calculations[57] and there is excellent agreement. From a value of 9.41 cm^{-1} for the *A* rotational constant an average value of 0.4 ps for the fastest rotational period of ketene at room temperature can be derived. So unless the dissociation is extremely fast (less than *ca.* 30 fs) significant rotation of the parent molecule between the initially photoselected plane and the plane at the instant of fragmentation will tend to smear out any non-equilibrium of Λ doublet population, if one were to exist for a non-rotating (cold) parent ketene molecule. The fastest real-time single-photon state-to-state dissociation lifetime measured for ketene is 19 ps[12] at a wavelength of 280 nm and this is many times the rotational period of a room-temperature sample of ketene.

In contrast with the clearly equivalent Λ doublet populations of CH in the 279.3 nm photolysis above, there is evidently a slight degree of orbital alignment in favour of Π (A′) symmetry for rotational levels of CH produced in the two-photon dissociation at 308 nm (Fig. 4). Although the degree of orbital alignment is not large (<0.2 for $N'' = 10$ and $N'' = 12$) it immediately poses the two questions of why there is alignment and why there is a discrepancy with the behaviour observed for dissociation at 279.3 nm. The answers are not at all clear. Possibly there are different dissociation processes dependent on available energy or the existence of two different, but close-lying, electronic states of the postulated formylmethylene intermediate where the 308 nm pathway produces CH with a degree of alignment that out-of-plane rotation of the parent molecule does not completely remove even at room temperature. It should be noted that at 308 nm a weak feature appears in the REMPI spectrum of CH_2CO [25] and may be indicative of a Rydberg state existing at this two-photon energy. There may be a dissociation process moving towards a completely unconstrained cleavage of the H—C—C bond, following predictions of the model of Bronikowski and Zare[72] which has been developed to account for the 2 : 1 ratio of Π (A′) : Π (A″) Λ doublet propensities in $^2\Pi$ products of bimolecular reactions $A + BC \rightarrow AB + C$, but to extrapolate this to the photodissociation (rather than reaction) under consideration here would assume first, that the lone π orbital on the CH arises from the breaking of the C—C bond and secondly, and unlikely for dissociation from a specifically prepared reagent, that fragmentation of this bond is equally likely from any angular orientation of H—C—C.

We comment finally on the observations of spontaneous fluorescence from the CH (A and B) states. The minimum energy required to produce these excited fragments corresponds to the absorption of at least three-photons, and the observed quadratic dependence of the fluorescence upon laser intensity shows that for a three-photon process, one step must be saturated. Fig. 2 shows the markedly different wavelength dependence for the two processes, showing that they cannot originate from the same photodissociation process. Unequal Λ doublet populations in the *N′* levels of the $^2\Delta$ state have been observed by Luque *et al.*[32] (for a photolysis wavelength of 193 nm) and the ratio demonstrated to depend upon *N′*. These authors suggest that multiphoton dissociation of the $^1CH_2$ product could be responsible for the formation of $CH(A\,^2\Delta)$; in the present experiments at longer photolysis wavelengths this cannot be so, as such a process, unsaturated in the first absorption step to the $^1A''$ state of ketene, could not yield a quadratic energy dependence if followed by a true two-photon absorption by singlet methylene.

M. R. H. gratefully acknowledges the SERC for the award of a maintenance grant.

References

1 R. G. W. Norrish, H. G. Crane and O. Saltmarsh. *J. Chem. Soc.*, 1933, 1533.
2 G. B. Porter, *J. Am. Chem. Soc.*, 1957, **79**, 827.
3 A. H. Laufer, *J. Phys. Chem.*, 1969, **73**, 959.
4 T. W. Eder and R. W. Carr, *J. Phys. Chem.*, 1969, **73**, 2074.
5 P. M. Kelley and W. L. Hase, *Chem. Phys. Lett.*, 1975, **35**, 57.
6 H. Bitto, D. R. Guyer, W. F. Polik and C. B. Moore, *Faraday Discuss., Chem. Soc.*, 1986, **82**, 149.
7 I-C. Chen, W. H. Green, and C. B. Moore, *J. Chem. Phys.*, 1988, **89**, 314.
8 W. H. Green, I-C. Chen and C. B. Moore, *Ber. Bunsenges. Phys. Chem.*, 1988, **92**, 389.
9 C. C. Hayden, D. M. Neumark, K. Shobatake, R. K. Sparks and Y. T. Lee, *J. Chem. Phys.*, 1982, **76**, 3607.
10 D. J. Nesbitt, H. Petek, M. F. Foltz, S. V. Filseth, D. J. Bamford and C. B. Moore, *J. Chem. Phys.*, 1985, **83**, 223.
11 W. H. Green, A. J. Mahoney, Q-K. Zheng and C. B. Moore, *J. Chem. Phys.*, 1991, **94**, 1961.
12 E. D. Potter, M. Gruebelle, L. R. Khundkar and A. H. Zewail, *Chem. Phys. Lett.*, 1989, **164**, 462.
13 S. J. Klippenstein and R. A. Marcus, *J. Chem. Phys.*, 1989, **91**, 2280.
14 S. J. Klippenstein and R. A. Marcus, *J. Chem. Phys.*, 1990, **93**, 2418.
15 B. I. Sonobe and R. N. Rosenfeld, *J. Am. Chem. Soc.*, 1983, **105**, 7528.
16 G. T. Fujimoto, M. E. Umstead and M. C. Lin, *Chem. Phys.*, 1982, **65**, 197.
17 K. G. Unfried, G. P. Glass and R. F. Curl, *Chem. Phys. Lett.*, 1991, **177**, 33.
18 X. Liu, S. G., Westre, J. D. Getty and P. B. Kelly, *Chem. Phys. Lett.*, 1992, **188**, 42.
19 W. D. Allen and H. F. Schaeffer III, *J. Chem. Phys.*, 1986, **84**, 2212.
20 W. D. Allen and H. F. Schaeffer III, *J. Chem. Phys.*, 1988, **89**, 329.
21 P. Chen, J. B. Pallix, W. A. Chupka and S. D. Colson, *J. Chem. Phys.*, 1986, **84**, 527.
22 J. B. Pallix, P. Chen, W. A. Chupka and S. D. Colson, *J. Chem. Phys.*, 1986, **84**, 5208.
23 P. Chen, J. B. Pallix, W. A. Chupka and S. D. Colson, *J. Chem. Phys.*, 1987, **86**, 516.
24 J. W. Hudgens, C. S. Dulcey, G. R. Long and D. J. Bogan, *J. Chem. Phys.*, 1987, **87**, 4546.
25 M. N. R. Ashfold, A. D. Couch, R. N. Dixon and B. Tutcher, *J. Phys. Chem.*, 1988, **92**, 5327.
26 M. R. Berman and M. C. Lin, *J. Chem. Phys.*, 1984, **81**, 5743.
27 K. H. Becker, B. Engelhardt, P. Wiesen and K. D. Bayes, *Chem. Phys. Lett.*, 1989, **154**, 342.
28 R. G. Macdonald and K. Liu, *J. Chem. Phys.*, 1989, **91**, 821.
29 C. Chen, Q. Ran, S. Yu and X. Ma, *Chem. Phys. Lett.*, 1993, **203**, 307.
30 F. Stuhl, personal communication, 1990.
31 T. Nagata, M. Suzuki, K. Suzuki, T. Kondow and K. Kuchitsu, *Chem. Phys.*, 1984, **88**, 163.
32 J. Luque, J. Ruiz and M. Martin, *Chem. Phys. Lett.*, 1993, **202**, 179.
33 G. Hancock and M. R. Heal, *J. Chem. Soc., Faraday Trans.*, 1992, **88**, 2121.
34 Z. Bembernek, R. Kepa, A. Para, M. Rytel, M. Zachwieja, G. J. Janjic and E. Marx, *J. Mol. Spectrosc.*, 1990, **139**, 1.
35 J. W. Williams and C. D. Hurd, *J. Org. Chem.*, 1940, **5**, 122.
36 A. H. Laufer and R. A. Keller, *J. Am. Chem. Soc.*, 1971, **93**, 61.

37 P. Bernath, *J. Chem. Phys.*, 1987, **86**, 4838.
38 J. M. Brown, J. T. Hougen, K. P. Huber, J. W. C. Johns, I. Kopp, H. Lefebrve-Brion, A. J. Merer, D. A. Ramsay, J. Rostas and R. N. Zare, *J. Mol. Spectrosc.*, 1975, **55**, 500.
39 M. H. Alexander, P. Andresen, R. Bacis, R. Bersohn, F. J. Comes, P. J. Dagdigian, R. N. Dixon, R. W. Field, G. W. Flynn, K. H. Gerricke, E. R. Grant, B. J. Howard, J. R. Huber, D. S. King, J. L. Kinsey, K. Kleinermans, K. Kuchitsu, A. C. Luntz, A. J. McCaffery, B. Pouilly, H. Reisler, S. Rosenwaks, E. W. Rothe, M. Shapiro, J. P. Simons, R. Vasudev, J. R. Wiesenfeld, C. Wittig and R. N. Zare, *J. Chem. Phys.*, 1988, **89**, 1749.
40 P. Andresen and E. W. Rothe, *J. Chem. Phys.*, 1985, **82**, 3634.
41 P. Andresen, G. S. Ondrey, B. Titze and E. W. Rothe, *J. Chem. Phys.*, 1984, **80**, 2548.
42 C. E. Moore and H. P. Broida, *J. Res. Natl. Bur. Stand. (U.S.), A*, 1959, **63**, 19.
43 R. L. Nuttall, A. H. Laufer and M. V. Kilday, *J. Thermodyn.*, 1971, **3**, 167.
44 M. W. Chase, C. A. Davies, J. R. Downey, D. J. Frurip, R. A. Macdonald and A. N. Syverud, *J. Phys. Chem. Ref. Data*, 1985, **14**.
45 G. Herzberg and J. W. C. Johns, *Proc. R. Soc. London, A*, 1966, **295**, 107.
46 I. Botterud, A. Lofthus and L. Veseth, *Phys. Scr.*, 1973, **8**, 218.
47 P. Andresen and E. W. Rothe, *J. Chem. Phys.*, 1983, **78**, 989.
48 P. Andresen, G. S. Ondrey and B. Titze, *Phys. Rev. Lett.*, 1983, **50**, 486.
49 A. U. Grunewald, K. H. Gericke and F. J. Comes, *Chem. Phys. Lett.*, 1987, **133**, 501.
50 K. H. Gericke, R. Theinl and F. J. Comes, *Chem. Phys. Lett.*, 1989, **164**, 605.
51 K. P. Huber and G. Herzberg, *Constants of Diatomic Molecules*, Van Nostrand Reinhold, New York, 1979.
52 H. Reisler and C. Wittig, *Annu. Rev. Phys. Chem.*, 1986, **37**, 307.
53 R. L. Russell and F. S. Rowland, *J. Am. Chem. Soc.*, 1970, **92**, 7508.
54 D. C. Montague and F. S. Rowland, *J. Am. Chem. Soc.*, 1971, **93**, 5381.
55 E. R. Lovejoy, S. K. Kim, R. A. Alvarez and C. B. Moore, *J. Chem. Phys.*, 1991, **95**, 4081.
56 W. J. Bouma, R. H. Nobes, L. Radom and C. E. Woodward, *J. Org. Chem.*, 1982, **47**, 1869.
57 K. Tanake and M. Yoshimine, *J. Am. Chem. Soc.*, 1980, **102**, 7655.
58 C. Vacek, B. T. Colegrove and H. F. Schaeffer III, *Chem. Phys. Lett.*, 1991, **177**, 468.
59 R. S. Mulliken, *Rev. Mod. Phys.*, 1931, **3**, 89.
60 J. Brzozowski, P. Bunker, N. Elander and P. Erman, *Astrophys. J.*, 1976, **207**, 414.
61 K. H. Becker, H. H. Brenig and T. Tatarczyk, *Chem. Phys. Lett.*, 1980, **71**, 242.
62 M. Ortiz and J. Campos, *Physica C*, 1982, **114**, 135.
63 W. Bauer, B. Engelhardt, P. Wiesen and K. H. Becker, *Chem. Phys. Lett.*, 1989, **158**, 321.
64 R. Schinke, *Annu. Rev. Phys. Chem.*, 1988, **39**, 39.
65 R. Schinke, *J. Phys. Chem.*, 1986, **90**, 1742.
66 D. J. Bamford, S. V. Filseth, M. F. Foltz, J. W. Hepburn and C. B. Moore, *J. Chem. Phys.*, 1985, **82**, 3032.
67 A. U. Grunewald, K. H. Gericke and F. J. Comes, *J. Chem. Phys.*, 1988, **89**, 345.
68 N. Sivakumar, G. E. Hall, P. L. Houston, J. W. Hepburn and I. Burak, *J. Chem. Phys.*, 1988, **88**, 3692.
69 R. Vasudev, R. N. Zare and R. N. Dixon, *J. Chem. Phys.*, 1984, **80**, 4863.
70 U. Bruhlmann, M. Dubs and J. R. Huber, *J. Chem. Phys.*, 1987, **86**, 1249.
71 J. W. C. Johns, J. M. R. Stone and G. Winnewisser, *J. Mol. Spectrosc.*, 1972, **42**, 523.
72 M. J. Bronikowski and R. N. Zare, *Chem. Phys. Lett.*, 1990, **166**, 5.

Paper 3/04863B; *Received* 11*th August*, 1993